Proceedings of DETC'03
ASME 2003 Design Engineering Technical Conferences and Computers and Information in Engineering Conference
Chicago, Illinois USA, September 2-6, 2003

DETC2003/DAC-48775

PARAMETERIZATION STRATEGY FOR OPTIMIZATION OF SHAPE MORPHING COMPLIANT MECHANISMS USING LOAD PATH REPRESENTATION

Kerr-Jia Lu
Department of Mechanical Engineering
University of Michigan
Ann Arbor, Michigan 48109
USA
Phone: 734-763-4916
Email: kjlu@umich.edu

Sridhar Kota
Department of Mechanical Engineering
University of Michigan
Ann Arbor, Michigan 48109
USA
Phone: 734-763-4916
Email: kota@umich.edu

ABSTRACT

The distributed compliance and smooth deformation field of compliant mechanisms provide a viable means to achieve shape morphing in many systems, such as flexible antenna reflectors and morphing aircraft wings. We previously developed a systematic synthesis approach to design shape morphing compliant mechanisms using Genetic Algorithm (GA). However, the design variable definition, in fact, allows the generation of invalid designs (disconnected structures) within the GA. In this research, we developed a load path representation to include the structure connectivity information into the design variables, thus improving the GA efficiency. The number of design variables is also independent of the number of elements in the finite element model that is used to solve for the structural deformation. The shape morphing synthesis approach, incorporating this path representation, is demonstrated through two examples, followed by discussions on further refinements.

Keywords: compliant mechanism, shape morphing, genetic algorithm, load path representation.

INTRODUCTION

Typical topology optimization for compliant mechanisms and structures involves the discretiztion of the design domain with finite element meshes, using either 2-dimensional quadrilateral (QUAD) elements in the continua approach [1, 2] or a network of truss/beam elements the grounded structure approach [3-7]. This discretization not only facilitates the use of finite element analysis (FEA) to solve for the structural deformation, it also defines the design variables; that is, for each element, a corresponding topology variable is used to describe a physical quantity or geometry of the element. The topology is then determined by including or eliminating the elements through the optimization process. Majority of the previous research has been incorporating a continuous optimization method to search for the optimal compliant mechanism topology [1-6]. The topology variables are allowed to vary continuously between a lower bound (usually very close to zero) and an upper bound. A filtering scheme is then applied to eliminate elements with topology values under a threshold value. The elimination of elements creates voids in the continua or changes the structure connectivity, which in turn varies the topology. However, the elimination becomes ambiguous when the variables take on intermediate values. In addition, the final design somewhat depends on the initial discretization resolution (mesh size); the finer the resolution is, the more design variables there are. Different discretization resolution can also lead to different optimal topology for the same problem.

On the other hand, size and shape optimization for compliant mechanisms generally serves as a refinement step following the topology optimization. In other words, the structural topology is held fixed in this step, while the design variables are the dimensions of the structure. Similar to the topology optimization problem, the majority of previous research has been using continuous optimization methods to solve the size and shape optimization problem. Although this two-step synthesis approach (first topology, then dimensions) has yielded many successful designs, most of the reported examples are single-input single-output (SISO) systems. Very little attention has been directed to problems with multiple output points, such as a shape morphing problem, when considering all points on the compliant mechanism boundary. In general, the topology optimization is considered the qualitative aspect that determines the output 'direction,' and the dimensional optimization is considered the quantitative aspect such as maximizing the output 'magnitude.' Since shape morphing requires all output points on the boundary to simultaneously move in different directions with different amounts, the qualitative and quantitative aspects are coupled. Therefore, a unified approach should be developed to appropriately address these aspects simultaneously.

With the development in Genetic Algorithm (GA), GA has been employed in many engineering fields, including structural optimization. Many published papers in the mechanical, aerospace, and civil engineering field have been focusing on incorporating GA into structural optimization [8-12], but it has only been incorporated into the compliant mechanism area very recently [13-17]. Due to GA's ability to handle both continuous and discrete variables, the topology, sizing, and shape optimization issues have been addressed separately as well as simultaneously in these works. The presence and elimination of topology design variables can then be represented as 0 and 1 respectively, thus eliminating the ambiguous filtering process required when using continuous variables.

We previously developed a synthesis approach using GA to search for the optimal topology and dimensions (beam dimensions) of a shape morphing compliant mechanism [15, 16]. The approach incorporates a GA to simultaneously determine the topology and dimensions of elements in a beam-element grounded structure. Although the results demonstrated the feasibility of the approach, the one-to-one correspondence between a design variable and an element, in fact, allows the generation of 'invalid' designs (disconnected structures). In other words, the solution space actually contains invalid solutions that should be excluded by constraints. A penalty term was introduced to differentiate invalid/unstable designs from valid ones in our previous research [15, 16] as well as other published literatures in the structural optimization field [8-12]. However, checking for the constraint violation and penalizing invalid designs can be expensive, especially with increasing number of design variables. In this research, we developed a load path representation to include structural connectivity information into the design variables. This facilitates the detection and exclusion of invalid structures from the solution space, thus improving the GA performance.

A brief overview of the synthesis approach we previously developed [16] is given in the next section, including some discussions on invalid structures. The load path representation will be introduced in the methodology section.

OVERVIEW: SYNTHESIS APPROACH FOR SHAPE MORPHING COMPLIANT MECHANISMS

In an earlier paper [16], we developed a systematic synthesis approach for shape morphing compliant mechanisms, using a GA to simultaneously determine the topology and dimensions. It is assumed that (1) the shape-changing object will change from its initial profile to only one target profile, (2) the initial and target profiles are specified a priori, (3) the shape-changing object (antenna or an aircraft wing) is integrally attached to the compliant mechanism, and (4) the compliant mechanism has only a single external input actuator at a specified location. The actuator can be selected from a variety of ranges and types, such as electric motor or even the smart actuators, as long as the required motion and force can provided. Figure 1 gives a simple illustration of shape morphing using a compliant mechanism. The actuator provides a displacement or force input to the system and induces the structural deformation in the compliant mechanism. This deformation transforms the boundary shape from its initial state to the 'deformed' state, which, ideally, should be the same as the target shape. Therefore, the goal is to minimize the difference or 'shape deviation' between the deformed and target curves by optimizing the topology and dimensions of the compliant mechanism. The flowchart in Fig. 2 gives an overview of the synthesis approach we previously developed, including three major components: (1) the GA to search for the optimal compliant mechanism, (2) the Finite Element Analysis (FEA) to solve for the structural deformation, and (3) the curve comparison schemes to evaluate the performance of each design in GA. As shown in Fig. 3, a grounded structure is used to discretize the design domain into a beam-element network. For each beam element, a binary variable (hTop) is used to determine the topology, and a continuous variable (hDim) is used to describe the cross-section dimension. The resulting element cross-section, h, is the multiplication of hTop and hDim. When $hTop_i$ is 0, the i^{th} element gets eliminated regardless of the $hDim_i$ value; when $hTop_i$ is 1, the i^{th} element has a cross-section of $hDim_i$, thus allowing the topology and dimensional aspects to be addressed simultaneously.

Although GA can combine the topology and dimensional synthesis steps into one, unlike the gradient-based optimization methods, GA can not efficiently eliminate unnecessary elements. That is, sometimes the design obtained from GA can include extra elements that do not provide strain energy storage nor contribute to the structural stiffness. Furthermore, it is also shown that 'invalid' designs (disconnected structures) can be created within the GA evolution process, as shown in Fig. 4 ~ Fig. 6. Similar issues regarding invalid/unstable structures have also been encountered in other structural optimization research using GA [8-12]. A penalty terms is typically added to the objective function when invalid designs are created, but the computation time required to detect the connectivity can be expensive, leading to inefficiency in GA. In order to further improve the GA performance, it is essential to understand why disconnected structure can be generated. In fact, the generation of invalid structures is no surprise. Because the binary topology design variables are defined in the element level, they do not explicitly contain any information about the overall connectivity, which is in the structural level. The structural connectivity is unknown when a set of binary value is assigned to describe the topology of a design. An additional checking algorithm has to be used *after* a topology is created to detect the structural connectivity and penalize the design if invalid. Thus, the structural connectivity should be incorporated into the design variables to eliminate or accelerate the connectivity checking process.

Tai et al. proposed a morphological representation [13, 14, 18] for structural topology and dimensions. This representation incorporates the connectivity information into the design variables and separates the design variable definition from the finite elements. Although the approach was demonstrated through several examples, it is still restricted to 2-dimensional problems with only a single output. In this research, we develop a load path representation that can simultaneously address the topology, size, and shape aspects in shape morphing (multiple output) problems. This approach allows relative motion between cross segments (one section slides over the top of another section), which can potentially be expanded to create 3-dimensional designs. Furthermore, it incorporates an adaptive meshing generation scheme with beam elements, thus eliminating the image mapping step required in the morphological approach.

For more details on the overall synthesis approach for shape morphing compliant mechanisms (Fig. 2), interested readers should refer to Lu and Kota [16]. In the following section, we will focus on the load path representation for the topology and dimensions of a compliant mechanism. This representation will be incorporated into the approach by replacing the step shown bold in Fig. 2 to enhance the performance of this systematic synthesis approach for shape morphing compliant mechanisms.

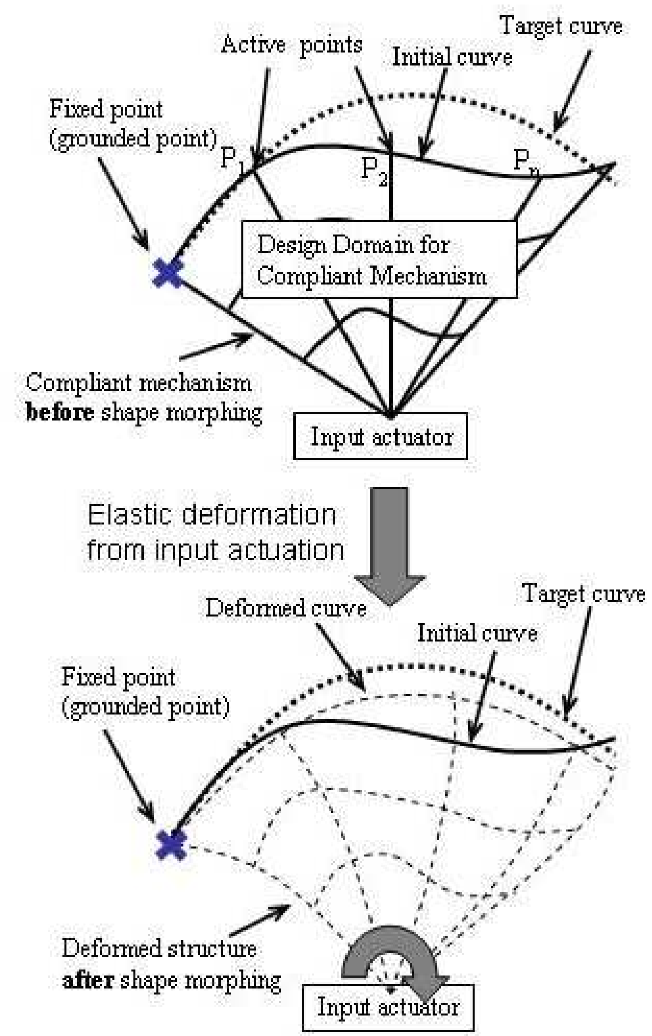

Figure 1: An illustration of a shape morphing compliant mechanism that changes the boundary shape from the initial state to the deformed shape [16].

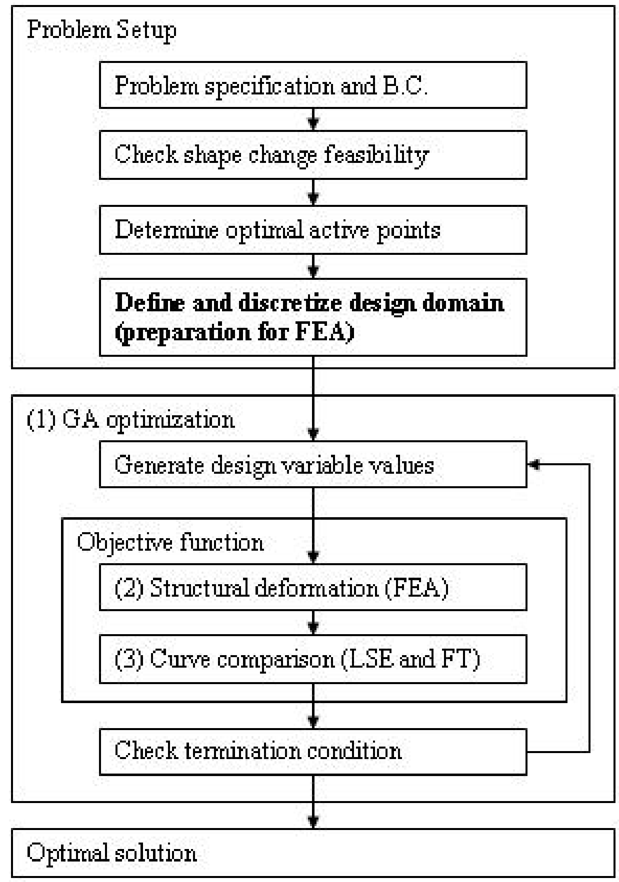

Figure 2: Flowchart of the synthesis approach for shape morphing compliant mechanisms [16].

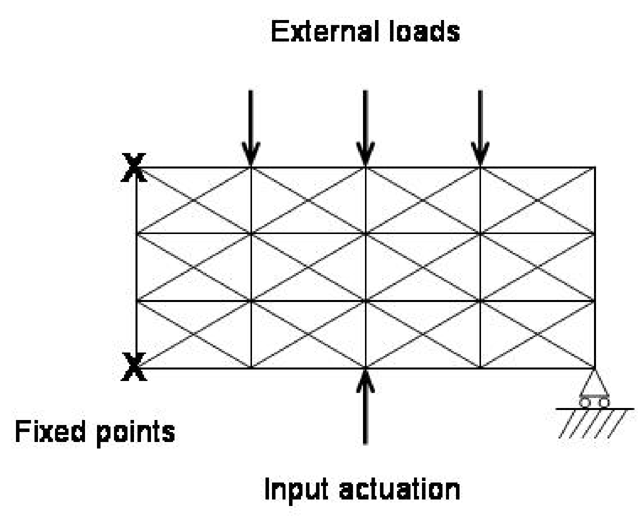

Figure 3: The design domain discretization using beam elements in a grounded structure approach.

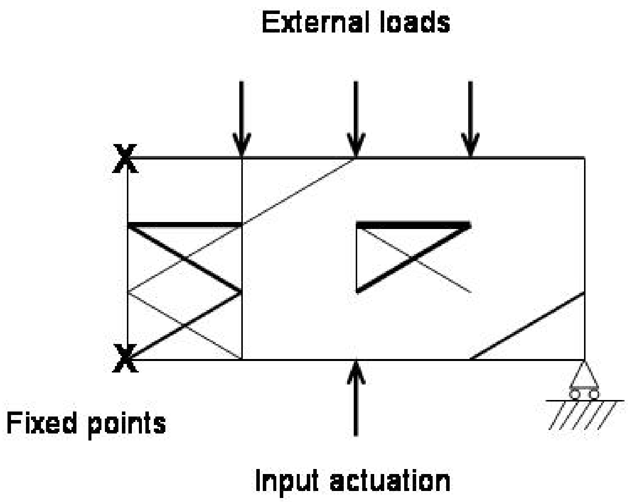

Figure 4: A disconnected sub-structure is generated when the elements all around are eliminated.

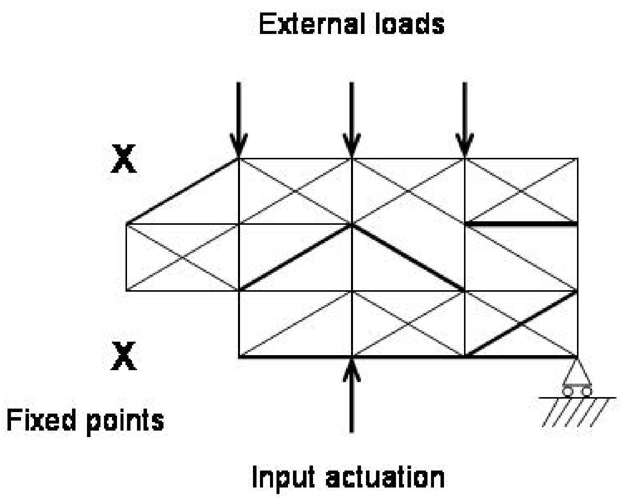

Figure 5: The structure has no connected to any fixed point, leading to rigid-body motions of the structure.

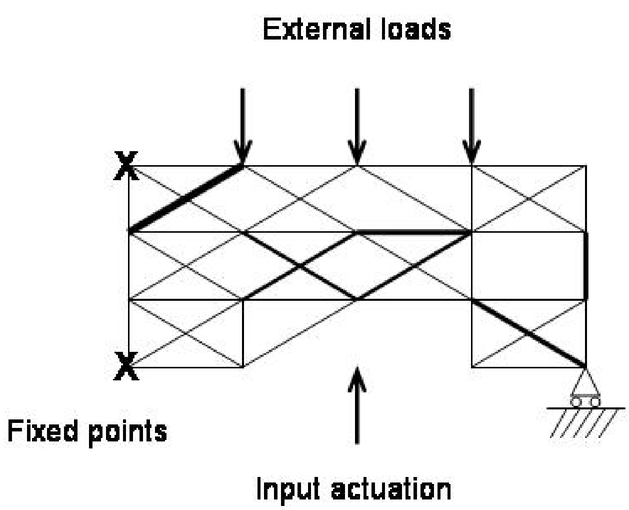

Figure 6: The input is disconnected from the structure, thus fail to achieve the desired motion.

METHODOLOGY

By observing various structures and compliant mechanisms, we found that there are two important requirements to avoid invalid designs: (1) input must be connected to one or more output points, and (2) the structure should be grounded at one or more points. These connections from input or fixed points to output points can be regarded as paths that deliver the energy from the input to the output points. Instead of using element geometries as design variables, these paths can be selected as the design variables that contain the structural connectivity information. Each path will have a corresponding set of dimension variables to describe the size and shape of the design. With this inspiration, we developed a load path representation for the topology and dimensional design variables to ensure all generated designs are properly connected.

Load Path Representation

In order to ensure the validity of all generated designs, we developed a load path representation to incorporate the connectivity information in the design variables. Typical single-input multiple-output (SIMO) compliant mechanisms have three common features: an input point, one or more output points, and at least one fixed point. These points should be connected either directly or indirectly to each other to generate a valid structure. In the load path representation, the topology of a compliant mechanism is represented with the load paths connecting the input/output/fixed points. As can be seen in Fig. 7, the fully connected structure includes three types of paths: from input to outputs, from input to fixed points, and from fixed points to output points. Note that the points are connected *directly* with the paths without any physical intermediate connections between different paths. However, direct connection between the points can limit the attainable topology connectivity. In order to increase the variety of available topologies, a set of grid points are used as the intermediate connection ports to allow additional connections between paths. These connection ports also enable a path to form loops and intersections with others to provide relatively rigid portions required in some designs. As shown in Fig. 8 and Table 1, all paths are now represented as a sequence of nodes, and the intermediate connection between paths can only occur at the connection ports. According to the connectivity of the design, ports 6, 7, and 11 are termed as active connection ports, while ports 8, 9, and 10 are inactive. The use of connection ports not only increases the variety of available topologies, but also allows relative motion between cross elements, which can potentially be expanded to generate three-dimensional topologies.

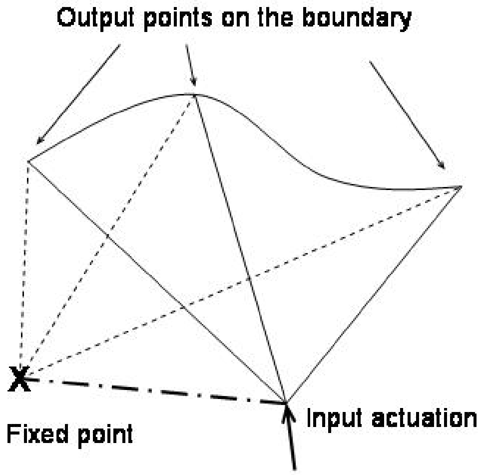

Figure 7: Three types of paths connecting the input, fixed point, and output, are shown in solid, center, and dash lines respectively.

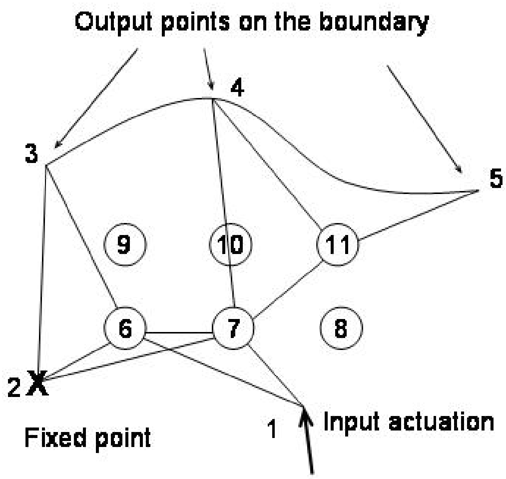

Figure 8: The load path representation of this example is shown in Table 1. Note that sections 1-6 and 2-7 are not physically connected.

Path #	Start point	End point	Path sequence
1	Input (1)	Output (3)	{1,6,3}
2	Input (1)	Output (4)	{1,7,11,4}
3	Input (1)	Output (5)	{1,7,11,5}
4	Input (1)	Fixed (2)	{1,6,2}
5	Fixed (2)	Output (3)	{2,3}
6	Fixed (2)	Output (3)	{2,6,7,4}
7	Fixed (2)	Output (5)	{2,7,11,5}

Table 1: The path sequences for the topology in Fig. 8.

Topology Design Variables

Most of the published literatures in structural topology optimization involve the discretization of the design domain into a finite element mesh with design variables assigned to each element. Unlike the element-design variable correlations in the previous research [1-7, 15, 16], the number of design variables in the load path representation is independent of the design domain resolution. The topology of the compliant mechanism is described by the connecting sequences of the paths and a corresponding binary variable ($pTop_i$) for each path. The binary variable, $pTop_i$, determines the presence ($pTop_i = 1$) or elimination ($pTop_i = 0$) of the i^{th} path. Figures 9 and 10 are two designs that have the same basic topology as the example in Fig. 8 ($pTop_i = 1$ for all paths) with some $pTop_i$ values set to zero. Their corresponding topology information can be found in Table 2.

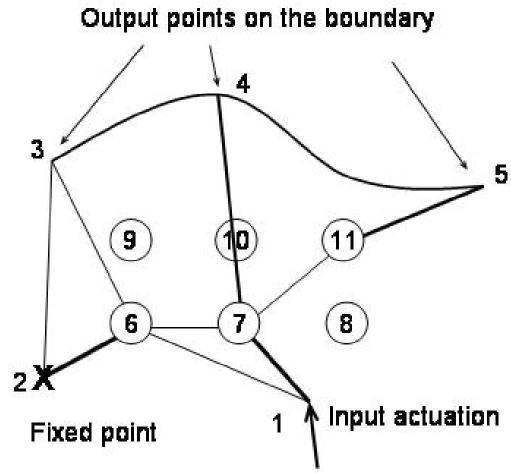

Figure 9: A new topology is obtained with the topology variables, $pTop_2$ and $pTop_7$, set to zero. The topology and dimensional information for this design can be found in Table 2 and Table 3 respectively.

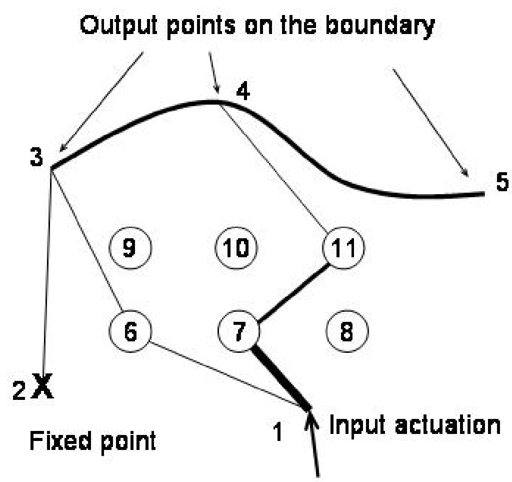

Figure 10: A new topology is obtained by changing the pTop values of the design in Fig. 8. The topology information is shown in Table 2.

Path #	Path seq.	$pTop_i$ Fig.9	$pTop_i$ Fig.10
1	{1,6,3}	1	1
2	{1,7,11,4}	0	1
3	{1,7,11,5}	1	0
4	{1,6,2}	1	0
5	{2,3}	1	1
6	{2,6,7,4}	1	0
7	{2,7,11,5}	0	0

Table 2: The topology information for the designs shown in Fig. 9 and Fig. 10.

Dimensional Design Variables

The dimensional variables, on the other hand, are the cross-section dimensions of the beam element connecting the paths. In this research, we are assuming linear beam elements with rectangular cross-sections. In addition, the cross-section remains constant between two consecutive connection ports. For a given path, there can be one or more 'sections,' depending on the length of the path sequence. A sequence of continuous variable, $pDim_i$, is assigned to each path to describe the in-plane beam dimensions, while the out-of-plane dimension is held fixed. Hence, the $pDim_i$ array is always one element shorter than the path sequence in length. The same example in Fig. 9 is used to illustrate the definition of dimensional variables with its topology and dimensional information listed in Table 3. As can be seen, each path has a corresponding $pDim_i$ string, but, due to the different $pTop_i$ values, some are not shown in the design. Note that some paths have overlapping sections with another path; for example, path #4 and #6 have an overlapping section between node 2 and 6 (shown bold in Table 3). That is, there are two different dimension values for this section, $pDim_4(2) = 1.3$ and $pDim_6(1) = 3$. Since only one value is required to describe the section dimension, one pDim value is randomly selected from the potential values (1.3 and 3 in this case) with uniform probability. The selected dominant value will, then, overwrite the other values.

In addition to the path section dimensions ($pDim_i$), another continuous variable, hBoundary, is used to represent the dimension of the boundary. In this research, it is assumed that the shape morphing boundary always exists in every design, and the boundary has a uniform cross-section. Therefore, it is unnecessary to assign a topology variable for the boundary, and only one dimensional variable is used to represent the boundary dimension.

Path #	Path seq.	$pTop_i$	$pDim_i$
1	{1,6,3}	1	{1,0.75}
2	{1,7,11,4}	0	{1,1,2}
3	{1,7,11,5}	1	{3,0.75,2.5}
4	{1,**6,2**}	1	{2.5,**1.3**}
5	{2,3}	1	{0.75}
6	{**2,6**,7,4}	1	{**3**,1.5,2.25}
7	{2,7,11,5}	0	{1.8,1,1}

Table 3: The topology and dimensional information for the design shown in Fig. 9.

Shape Design Variables: Connection Port Locations

As opposed to the fixed FEA mesh approach used in previous research [15, 16], the design resolution can be varied through changing the connection port locations in the load path representation. All the connection ports are allowed to move within a specified common region. Thus, their locations can be regarded as the shape variables. While the connectivity between the connection ports determines the topology of a compliant mechanism, the locations of them determines 'shape' of the path. Figure 11 shows a design having the same topology as that in Fig. 9. By merely changing the locations of two active connection ports (6 and 7), the two designs now have very different appearances. As can be seen, the two designs have the same connectivity but different section lengths and orientations.

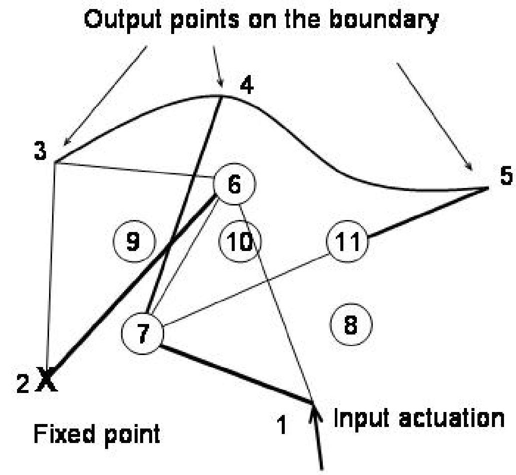

Figure 11: A design having the same topology as that in Fig. 9 but different connection port locations (port #6 and #7).

Constraints

By studying the problematic topologies shown in Fig. 4 ~ Fig. 6, we found two basic requirements for a valid design: (1) the structure needs to be grounded with one or more fixed points, and (2) the input has to be connected to the rest of the structure. These rules can easily be incorporated in the path representation parameterization by monitoring the $pTop_i$ values of paths from input and fixed point to the output points. At least one of the $pTop_i$ values in each path category has to be 1. This is a huge advantage over the grounded structure approach (Fig. 3), where a topology variable only determines the existence of *one* element. The connections (paths) between the input/fixed points to the output points are explicitly shown in the $pTop_i$ variables, whereas this connection information has to be 'searched for' in the grounded structure approach. In addition to the two validity requirements (constraints), a stress constraint is applied to prevent yielding in the compliant mechanism, and a strength constraint is used as a stiffness requirement for the structure to withstand external loads.

Adaptive Finite Element Mesh and Curve Comparison

The objective for the optimization is to find the optimal topology and dimensions for the compliant mechanism that can achieve the desired shape change with minimum error. To evaluate the 'performance' of each design, we used the Least Square Error (LSE) formulated previously to find the 'shape deviation.' The deviation is measured based on the sampling points on the deformed and target curves illustrated in Fig. 12. The target curve is the desired profile after shape morphing, while the deformed curve is what a particular compliant mechanism actually achieves with the input actuation. The structural deformation is solved for using a finite element analysis (FEA). As opposed to the fixed mesh used in most of the previous research [15, 16], the FE mesh is generated *after*

GA determines the design variables in the evolution process. Although the mesh is different for each design, an adaptive mesh using beam elements can actually be implemented quite easily using the path/dimension information in the design variables. The deformed structural boundary information is then extracted and compared with the target curve to determine the LSE deviation.

The LSE deviation is defined in Eq. (1), using the sampling points on the deformed and target curves, $P_{TAR,i}$ and $P_{DEF,i}$. The smaller the deviation is, the closer the design can achieve the desired shape morphing. Interested readers should refer to Lu and Kota [16] for more details on the objective function formulation.

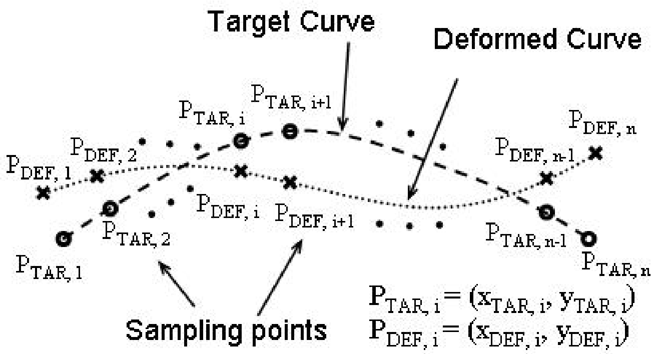

Figure 12: The deformed and target curves of a shape morphing compliant mechanism [16].

$$LSE_{deviation} = \frac{1}{n}\sum_{i=1}^{n}\sqrt{(x_{DEF,i} - x_{TAR,i})^2 + (y_{DEF,i} - y_{TAR,i})^2}\,, \qquad (1)$$

where n is the number of sampling points on each curve.

Optimization Problem

The optimization problem can be summarized in Eq. (2) ~ Eq. (11). The objective is to minimize the LSE deviation between the deformed and target boundary profiles. The equilibrium condition is satisfied through the use of FEA, shown in Eq. (3). The beam element dimensions (in-plane) are constrained between a minimum and a maximum values, typically based on the manufacturing constraints, shown in Eq. (4) and Eq. (5). Equation (6) shows the beam dimensions, resulting from the topology and dimensional design variables. The locations of the connection ports are allowed to wander within a specified range, as shown in Eq. (7). The validity (connectivity) requirements, Eq. (8) and Eq. (9), are also included in the constraints to ensure all the generated designs are properly connected. A stress constraint in Eq. (10) is imposed on all the elements. As seen in Eq. (11), the stiffness is achieved by constraining the maximum nodal displacement to stay within an acceptable value, when the actuator is inactive (blocked). The optimization problem is then solved with a genetic algorithm to handle discrete and continuous variables.

Objective Function

$$\min_{pTop_i,\, pDim_i,\, hBoundary,\, portLocation} \left(LSE_{deviation}\right) \qquad (2)$$

Subject to

$$\mathbf{d} = \mathbf{K}^{-1}\mathbf{F} \qquad (3)$$

$$pDim_{\min} < pDim_{i,j} \le pDim_{\max} \qquad (4)$$

$$pDim_{\min} < hBoundary \le pDim_{\max} \qquad (5)$$

$$h_e = pTop_i \times pDim_{i,j} \qquad (6)$$

$$(x_{\min}, y_{\min}) \le portLocation \le (x_{\max}, y_{\max}) \qquad (7)$$

$$\sum_{i \in pathInOut} pTop_i \ge 1 \qquad (8)$$

$$\sum_{i \in pathFixOut} pTop_i \ge 1 \qquad (9)$$

$$\sigma_e \le \sigma_{allowable} \qquad (10)$$

$$\max(d_{unactuated}) \le d_{allowable} \qquad (11)$$

where pTop $\in$ {0,1};

pDim, hBoundary, portLocation $\in \mathbb{R}^+$;

i: path number;

j: section number in the ith path;

e: number of elements.

Implementation in GA: Crossover and Mutation

Crossover and mutation are two genetic operations commonly seen in GA. The crossover and mutation strategies determine the varieties of designs that can be generated in the GA process. Typical GA represents the design variables into a string, analogous to the genes located on the DNA. The crossover is usually done by exchanging one or more segments between two chromosome strings. On the other hand, the mutation is done by altering one randomly selected element in the chromosome string. However, for a more complicated design variable data structure, such as the load path representation, the crossover and mutation strategies have to be more sophisticated. We, therefore, developed several simple strategies to work with the representation in this research.

With the load path representation method, the crossover strategy in this approach is to ‘exchange’ the path sequence, pTop, and pDim information of several randomly selected paths within two parent designs. This process produces new topology connectivity and changes the section dimensions at the same time. With the new path sequence information, new active/inactive connection ports can be generated. When a new active connection port is generated, a new port location is randomly selected within the design domain. In addition, the boundary dimension (hBoundary) of the two parent designs can be exchanged according to the crossover probability.

For the mutation process, the boundary dimension is replaced by a randomly generated value within the upper and lower bounds. In addition, the destinations (end points) of some randomly selected paths can mutate to a different one within the same category. For example, a path originally connecting the input to one of the output points can be mutated into a path connecting the input to another output point, simply by changing the last component in the path sequence.

RESULTS

Flexible antenna and aircraft wings are two application areas where shape morphing can potentially enhance the system performance and increase flexibility. A flexible antenna reflector and a morphing aircraft trailing edge are shown in this section to illustrate this synthesis approach.

Antenna Reflector Beam Steering

Figure 13 is an example of antenna reflector in its beam-steering mode that changes the orientation of the reflector, and, in turn, varies the coverage area. In this example, we design a compliant mechanism that is capable of simulating a rigid body rotation about the center. The GA starts with an initial population of 100 individuals and allows 80 generations, while the crossover and mutation probabilities are 0.8 and 0.3 respectively. As shown in Fig. 13, the shape morphing is achieved with an input of 2mm (0.0787inch) in the negative x-direction, while the top boundary is subjected to a constant load of 1N (0.2248lbf) downwards. The resulting LSE deviation is 1.2287mm (0.05inch) with a maximum stress of 22.32MPa (3237.82psi), less than the yielding stress for ABS, 34.45MPa (4996.55psi). The required actuation force is around 4.58N (1.03lbf) to the left and the maximum $d_{unactuated}$ in Eq. (10) is 0.63mm (0.025inch). The horizontal dimension of this antenna model is 200mm (7.874inch), and the vertical dimension is 30mm (1.181inch). Maximum deflection is 8.24mm (0.32inch) upwards at the left tip. The minimum and maximum in-plane beam dimensions are 1.99mm (0.078inch) and 2.76mm (0.11inch) respectively, and the out-of-plane dimension is 4mm (0.1575inch) in this design. The CPU time is about 5 minutes.

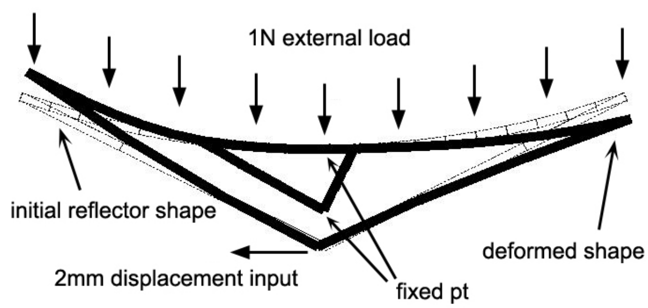

Figure 13: Two ends of the antenna reflector are required to bend upwards and downwards to simulate a change in orientation of 3° clockwise.

Aircraft Trailing Edge Shape Morphing

Most aircraft wings are optimized to produce minimum drag under a particular flying speed, at which the largest proportion of fuel is expended. However, in reality, flying speed varies continuously throughout flight. Hence, to obtain optimal fuel efficiency, the wing shape should be able to change in response to the change in flying speed [15]. As shown in Fig. 14, we design a compliant trailing edge that is able to deflect 10 degrees downwards to enhance the handling and maneuvering capabilities. The GA starts with an initial population of 80 and allows 80 generations, while the crossover and mutation probabilities are 0.8 and 0.3 respectively. The shape morphing is achieved with an input of 50.8mm (2inch) displacement at an angle of -11.4287 degrees without any external load. The resulting LSE deviation is 12.76mm (0.50217inch), while the maximum stress is 227.45MPa (32989psi), less than the yielding stress for aluminum, 227.53MPa (33000psi). The required actuation force is around 78.38N (17.62lbf). The horizontal dimension for this model is 889mm (35inch) and the vertical dimension is 381mm (15inch). Maximum deflection is 115.47mm (6.121inch) downwards at the tip of the trailing edge. In addition, the minimum and maximum in-plane beam dimensions are 1.3208mm (0.052inch) and 2.982mm (0.1174inch) respectively, and the out-of-plane dimension is 25.4mm (1inch). The CPU time is roughly 2 minutes.

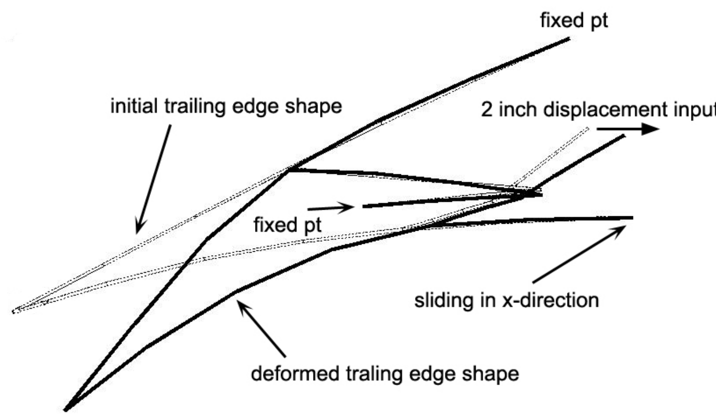

Figure 14: The trailing edge is required to deflect 10 degrees downwards.

DISCUSSIONS

Number of Design Variables and Design Resolution

As opposed to using each finite element dimension as a design variable, the load path representation utilizes the intermediate connection ports to define the topology and shape. The sizing aspect, on the other hand, is determined by the path sections constructing the topology. Therefore, the number of design variables, including the connection ports and path section dimensions, is reduced and is independent of the resolution of the final design. This eliminates the need to pre-specify the mesh resolution typically defined during the design domain discretization.

Convergence to Local Optimum

As seen in Fig. 13 and Fig. 14, the desired shape morphing can be achieved with the optimal compliant mechanism obtained from the GA. Although some minor errors can still be seen in the examples, we suspect that it is because the obtained design is not exactly a local optimum. In fact, this is one of the drawbacks using GA. Due to its heuristic property, GA can efficiently search in a large solution space, but converging to a local optimum can be quite difficult. However, we believe the designs in Fig. 13 and Fig. 14 are very close to the local optima nearby. The shape deviation can be further reduced if a gradient-based local search is implemented following the GA or embedded within the GA.

Boundary Conditions

It is observed that the locations of the fixed points are critical to the solution, because they provide points which the whole structure pivots about. In fact, the topology of a compliant mechanism not only includes the connectivity of the nodes, but it also includes the relative location of input, output, and fixed points, i.e. the boundary conditions. In this research, the locations of the fixed points are specified and fixed throughout the GA. The connectivity to the fixed points (boundary condition) is changed only when the pTop of a path to or from a fixed point is set to zero. However, the locations of the fixed points can be further incorporated into the shape design variables to study the effect of their locations.

Objective Function and Constraints

We previously developed two curve comparison schemes, using LSE and a modified Fourier Transformation (FT) [16]. However, all the examples shown in Fig. 13 and Fig. 14 are obtained using LSE deviation as the objective function. Although the modified FT can give similar results and even the mirror images, its calculation time is longer than that required for LSE deviation. Therefore, we believe LSE deviation is sufficient to evaluate the shape morphing effectiveness. In the GA, the constraints are implemented by adding penalty terms to the objective function. The major penalties in the shape change problem come from the violation of stress and stiffness constraints. Additional constraints, such as minimizing total volume or matching the actuation force with an existing actuator, can be included into the problem formulation; however, the original objective (minimizing shape deviation) can be obscured by these additional penalty terms. Thus, methods of handling multiple objectives or constraints in GA should be investigated to further enhance the performance of this synthesis approach.

SUMMARY

A load path representation is developed in this research as an alternative way to define the topology, size, and shape design variables in the structural optimization problems. It is incorporated into a systematic synthesis approach that we previously developed to find the optimal compliant mechanism for desired shape morphing. The load path representation allows the GA to efficiently detect the invalid designs and exclude them from the solution space, while maintaining sufficient design varieties. The results show that the compliant mechanisms obtained from GA can indeed achieve the desired shape morphing. The results also demonstrate the capability of the load path representation to create various designs with fewer design variables, compared to the grounded structure discretization approach. Furthermore, the binary path topology variable eliminates the filtering scheme associated with the use of continuous optimization method. In order to improve the convergence to a local optimum, we are currently incorporating a local search within or following the GA. At the same time, we are constantly exploring new applications that can potentially benefit from shape morphing compliant mechanisms.

ACKNOWLEDGMENTS

Authors gratefully acknowledge the funding support of U.S. Air Force Office of Scientific Research for this work under the research contract number F49620-96-1-0205.

REFERENCES

[1] Ananthasuresh, G.K., Kota, S. and Kikuchi, K., 1994, "Strategies for Systematic Synthesis of Compliant MEMS," ASME Winter Annual Meeting, ASME, Vol. 55, pp. 677-686.

[2] Nishiwaki, S., Frecker, M.I., Min, S. and Kikuchi, N., 1998, "Topology Optimization of Compliant Mechanisms Using the Homogenization Method," International Journal for Numerical Methods in Engineering, **42**(3)**,** pp. 535-559.

[3] Kota, S., Hetrick, J., Li, Z. and Saggere, L., 1999, "Tailoring Unconventional Actuators Using Compliant Transmissions: Design Methods and Applications," IEEE/ASME Transactions on Mechatronics, **4**(4)**,** pp. 396-408.

[4] Frecker, M., Kikuchi, K. and Kota, S., 1999, "Topology Optimization of Compliant Mechanisms with Multiple Outputs," Structural Optimization, **17**(4)**,** pp. 269-278.

[5] Hetrick, J. and Kota, S., 1999, "An Energy Formulation for Parametric Size and Shape Optimization of Compliant Mechanisms," ASME Journal of Mechanical Design, **121,** pp. 229-234.

[6] Joo, J., Kota, S. and Kikuchi, N., 2001, "Nonlinear Synthesis of Compliant Mechanisms: Topology Design," 2001 ASME Design Engineering Technical Conferences, ASME, Pittsburgh, PA, DETC2001/MECH-14141.

[7] Kota, S., Joo, J., Li, Z., Rodgers, S.M. and Sniegowski, J., 2001, "Design of Compliant Mechanisms: Applications to MEMS," Analog Integrated Circuits and Signal Processing, **29**(1-2)**,** pp. 7-15.

[8] Deb, K. and Gulati, S., 2001, "Design of Truss-Structures for Minimum Weight Using Genetic Algorithms," Finite Elements in Analysis and Design, **37**(5)**,** pp. 447-465.

[9] Chapman, C.D., Saitou, K. and Jakiela, M.J., 1994, "Genetic Algorithms as an Approach to Configuration and Topology Design," ASME Journal of Mechanical Design, **116,** pp. 1005-1012.

[10] Hajela, P. and Lee, E., 1998, "Genetic Algorithms in Truss Topological Optimization," International Journal of Solid Structures, **32**(22)**,** pp. 3341-3357.

[11] Rajan, S.D., 1995, "Sizing, Shape, and topology Design Optimization of Trusses Using Genetic Algorithm," Journal of Structural Engineering, **121**(10)**,** pp. 1480-1487.

[12] Shrestha, S.M. and Ghaboussi, J., 1998, "Evolution of Optimum Structural Shapes Using Genetic Algorithm," Journal of Structural Engineering, **124**(11)**,** pp. 1331-1338.

[13] Akhtar, S., Tai, K. and Prasad, J., 2002, "Topology Optimization of Compliant Mechanisms Using Evolutionary Algorithm with Design Geometry Encoded as a Graph," ASME 2002 Design Engineering Technical Conferences, ASME, Montreal, Canada, DETC2002/DAC-34147.

[14] Tai, K. and Chee, T.H., 2000, "Design of Structures and Compliant Mechanisms by Evolutionary Optimization of Morphological Representations of Topology," ASME Journal of Mechanical Design, **122,** pp. 560-566.

[15] Lu, K.J. and Kota, S., 2002, "Compliant Mechanism Synthesis for Shape-Change Applications: Preliminary Results," SPIE Modeling, Signal Processing, and Control Conference, SPIE, San Diego, Vol. 4693, pp. 161-172.

[16] Lu, K.J. and Kota, S., 2003, "Design of Compliant Mechanisms for Morphing Structural Shapes," Journal of Intelligent Materials Systems and Structures (in review).

[17] Parsons, R. and Canfield, S.L., 2002, "Developing Genetic Programming Techniques for the Design of Compliant Mechanisms," Structural and Multidisciplinary Optimization, **24,** pp. 78-86.

[18] Cui, G.Y., Tai, K. and Wang, B.P., 2002, "Topology Optimization for Maximum Natural Frequency Using Simulated Annealing and Morphological Representation," AIAA Journal, **40**(3)**,** pp. 586-589.